Digital Control and Phase Governing of Interleaved Multistage Hybrid Boost Capacitor Charger for Improved Efficiency and Power Density

Daniel Beniaminson*, *Student Member*, *IEEE,* Bar Halivni*, *Student Member*, *IEEE*, Michael Evzelman*, *Member*,*IEEE,* Alon Kuperman§, *Member*, *IEEE* and Mor Mordechai Peretz*, *Member*, *IEEE*

*The Center for Power Electronics and Mixed-Signal IC, Department of Electrical and Computer Engineering
Ben-Gurion University of the Negev, P.O. Box 653, Beer-Sheva, 8410501 Israel
benidani@post.bgu.ac.il, barhal@post.bgu.ac.il, evzelman@bgu.ac.il, morp@bgu.ac.il
http://www.ee.bgu.ac.il/~pemic

§Applied Energy Laboratory, Department of Electrical and Computer Engineering,
Ben-Gurion University of the Negev, P.O. Box 653, Beer-Sheva 84105, Israel
alonk@bgu.ac.il

***Abstract* – This paper introduces a digitally controlled multiphase multistage hybrid boost converter (MMHBC) for high voltage capacitor charging applications. Rapid capacitor charging control approach is presented, and topological variations to improve efficiency are examined. The controller provides tight output current regulation, while maintaining real-time current balancing capabilities for superior thermal distribution and converter efficiency. The MMHBC is capable of rapid capacitor bank charging to high voltage by forcing maximum output current at the first stage, which translates into maximal output power during the whole charging period. The controller includes a system governor unit which facilitates additional control aspects for multiphase operation such as phase shedding, soft-start mechanism, and system protection. SMPS operation, rapid capacitor charging, and topological improvements are validated experimentally on a four-phase 12V-to-300V multiphase prototype with a maximum output power of 250W and power density of 2.5kW/Liter.**

Keywords – Hybrid Boost, Digital Control, Capacitor Charger, Multiphase.

I. INTRODUCTION

A focal point of state-of-the-art SMPS is system miniaturization and obtaining higher overall system power density [1]-[5]. Smaller SMPS that maintain the same output power is the key to enabling power solutions that can be either implemented in mobile applications [6]-[7] or to increase the total power output for a given volume. The overall SMPS size in high conversion ratio boost type converters is highly dependent on the selected topology. Traditional solutions for high conversion ratio high-power SMPS include either resonant converters [8]-[10], or hard switched topologies [11]-[12], which often rely on a transformer to obtain the desired voltage gain. The implementation of such a high-power transformer requires substantial volume and therefore, increases system size and reduces the SMPS power density. Transformer-less boost-type topologies [13]-[15] eliminate the need for bulky magnetics to achieve the desired voltage conversion ratio that often comes at the cost of more complex design and components stress.

Another SMPS miniaturization technique is using multiphase converters. In multiphase converters with load sharing capabilities [16]-[18], each phase of the SMPS is required to provide less per-phase power, which translates into reduced components stress and size. Load sharing increases the system efficiency [19]-[21] and enables system scalability by adding additional phases if a higher power is required. Operating a multiphase system requires addressing additional control aspects beyond the traditional system's state-variable regulation. Phase synchronization and current balancing are required for the proper operation of the multiphase converter. In order to further improve the performance of the multiphase converters, phase shedding and phase interleaving [22]-[23] are used to enhance system efficiency over a wide range of loading conditions.

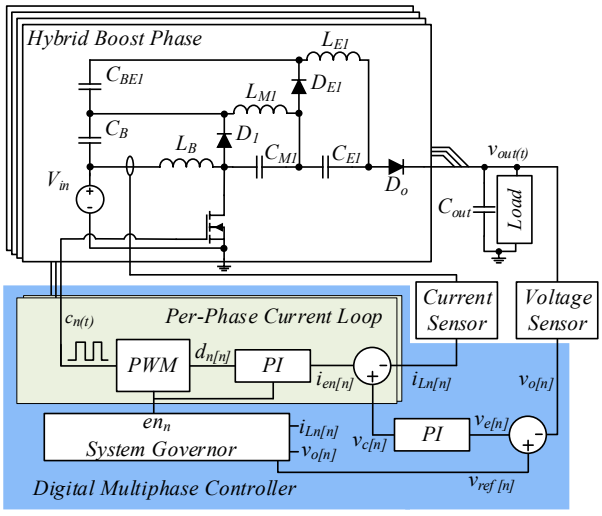

Fig. 1. Simplified schematic diagram of a transformer-less single-switch multiphase multistage boost converter with dual loop ACM controller.

The objective of this study is to introduce a digitally controlled multiphase multistage hybrid boost converter (MMHBC) for high voltage capacitor charging applications as shown in Fig. 1. The new multiphase converter utilizes an Average Current Mode (ACM) control scheme, which provides inherent current sharing and load-distribution capabilities among the phases. Due to the direct current control of each phase the converter is capable of rapidly charging large capacitive loads to high voltage at peak input power. The converter is implemented with transformer-less single-switch dual-inductor hybrid a hybrid boost phase with an additional amplification stage as shown in [15]. This paper further highlights the system governor which governs the capacitive load charging procedure and steady-state regulation, as well as additional control features to facilitate the multiphase converter architecture.

The rest of the paper is organized as follows, Section II describes the MMHBC operation and control scheme. Section III covers the operation and control features executed by the multiphase system governor. Experimental verification of the MMHBC is provided in section IV. Section V concludes the paper.

II. MMHBC ARCHITECTURE

A. Topology Overview

The high conversion ratio SMPS developed in this study which consists of a multiphase multistage hybrid boost converter and a multiphase digital dual-loop ACM controller is presented in Fig. 1. The digital controller is structured around a dual-loop current-programmed linear compensation scheme and operates in a fixed-frequency pulse width modulation. By operating under fixed frequency regime, it enables simpler power stage design procedure, requires only a relatively simple analog front-end and provides high static efficiency. Good thermal distribution between the phases is also obtained by maintaining balanced currents among the phases, which is highly important in the context of multiphase converters. The single-phase variation of two-stages hybrid boost converter [15] with dual-loop control scheme is demonstrated in Fig. 2. This topology was selected due to its highly efficient power conversion capabilities and low component stress in high conversion ratio applications which is achieved by low duty cycle signal due to the addition of the boost extension. Since this topology doesn't require the use of a bulky transformer to achieve the desired conversion ratio, a higher power density is feasible in comparison to other transformer-based topologies.

B. Controller Principle of Operation

In this study the dual-loop control architecture is implemented by a high bandwidth inner current loop that directly controls the boost stage inductor (L_B) current and a slower outer voltage loop that regulates the converter output voltage. In this study the inner current loop is realized by an ACM control approach, this is done to reduce the analog hardware requirements and the controller design complexity in comparison to a peak current mode controller implementation. The principle of operation of the introduced ACM controller is described with the aid of Fig. 3, which shows the conceptual block diagram of the ACM controller. Since this study focuses

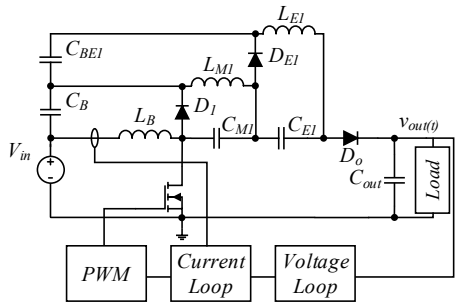

Fig. 2. Dual-loop single-phase two-stages hybrid boost converter.

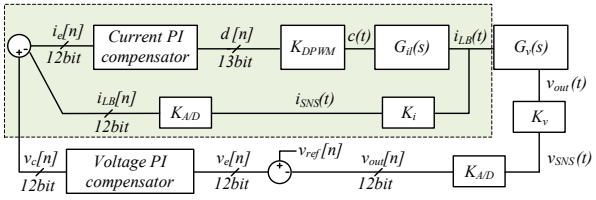

Fig. 3. Conceptual block diagram of the hybrid boost converter dual-loop ACM control system.

on a digital implementation of the controller, the description is carried out with sample-data domain notations. The outer voltage loop creates a digital reference $v_c[n]$ for the inner current loop based upon the error signal $v_e[n]$, which is calculated form the output voltage sampled voltage $v_{out}[n]$ and the voltage loop reference signal $v_{ref}[n]$.

The current error $i_e[n]$ can be calculated using the sampled average boost inductor current $i_{LB}[n]$ and the voltage loop digital reference. The current error $i_e[n]$ is fed as the input for the current loop compensator, which in turn generates the duty command $d[n]$ for the DPWM module, and a pulse width modulated signal $c(t)$ is formed.

The MMHBC configuration where multiple single-phase converters (Fig. 2) are connected to a single output stage, this requires minor adaptation of the control scheme to accommodate the additional phases and support load sharing between the phases. Active current balancing is required in multiphase operation to compensate for component non-idealities and practical implementation variation between the phases, these factors greatly increase the current mismatch between the phases when the same duty cycle command is applied to each phase. In the multiphase implementation of the ACM controller the inner current loop (inner frame of Fig. 3), which is described above, is multiplied on a per-phase basis. Each of the current loops are provided with the same $v_c[n]$ command, therefore the boost inductors currents $i_{LB}(t)$ are equalized by the control loops and current balancing is achieved. Since the per-phase current equalization is obtained inherently by the current loop operation no additional control loop is required.

Another aspect of the multiphase implementation of the MMHBC is the prevention of current flow back to either of the phases from the common output stage, making a specific phase an additional load instead of a power supply. This can also negatively affect system efficiency or cause system failure by overloading the remaining phases. This problem is solved

inherently by the hybrid boost converter topology with the implementation of D_o diode which prevents current backflow to the phase.

III. System Governor

In addition to the regulation requirements performed by the digital multiphase controller, unique control features such as phase shedding, soft-start, and protection attributes are required by the MMHBC controller. In this study all the additional control features are carried out by the system governor (Fig. 1). The phase shedding feature is responsible for optimizing the operational phases count according to the load status. By doing so the converter's efficiency can be increased in low, and medium load conditions where fewer phases can provide the desired load power while cutting back on drive losses.

A phase shedding and phase adding procedure, transitioning from a two-phase operation to a single-phase operation and back is demonstrated in Fig. 4. In this example phase 2 is shed in a governed manner to minimize the resultant output voltage deviation. The shedding procedure begins at t_s, from this time instance the current reference of phase 2 is gradually decreased to zero in order to reduce the phase inductors currents. During the shedding process of phase 2 the reference of phase 1 is increased to mitigate the reference reduction of phase 2. This stage lasts until the inductor currents are approximately zero, at this point (t_{fs}) the phases can be shed by setting phase 2 PWM signal to '0'. Due to the minimal energy stored in the reactive elements of the dropped phases, the output voltage remains almost constant during the shedding procedure. After the phase is shed, the load current is spread equally among the remaining phases increasing each phase average current from I_{pre} to I_{shd}. The phase adding procedure operates in a similar manner to the phase shedding case to control the current ramp up of phase 2. During this stage the phase 2 PWM signal is released at t_{add} back to the ACM controller to govern the current ramping. The current reference for phase 2 is increased until t_{fa} where the inductor currents are equal. After the phase adding is complete each phase currents are equal so the load is split equally.

Fig. 5. demonstrate the MMHBC fast capacitor charging procedure, where the converter operates at maximal power output to rapidly charge high capacitance load to high voltage. During the charging phase the converter operates at a constant current charging mode where each phase operates in its maximal current capability. The charging phase begin at t_s as the system governor halts the voltage compensator operation and sets the phases current reference to its peak value. Due to the current loop regulation the phases currents are constant while the output voltage rises. At the time instance where the output voltage reach its nominal value (V_{nom}) at t_{CV}, the system governor resets the voltage compensator and release the current references to maintain constant output voltage. This charging procedure ensure maximal power output to obtain the shortest charging time.

IV. Experimental Results

The digital multiphase controller introduced in this study has been validated using a 12V-to-300V four-phase MMHBC. An experimental prototype with all the analog front-end peripherals

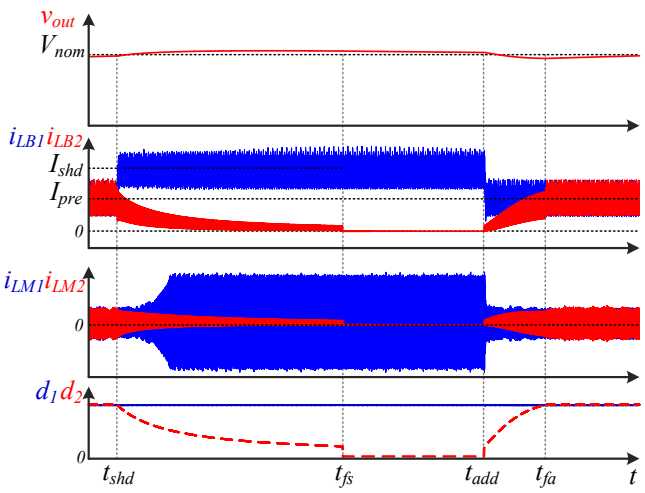

Fig. 4. Governed phase shedding and phase adding utilizing the dual loop controller architecture.

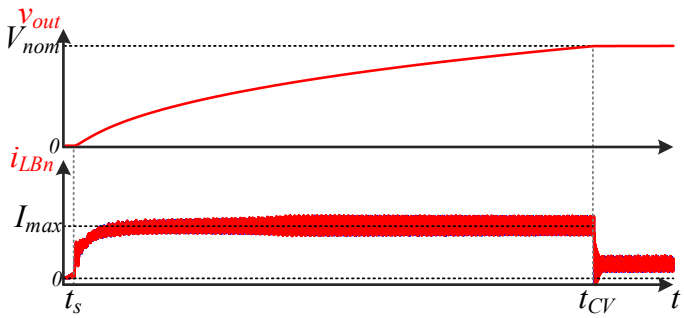

Fig. 5. Constant current mode high voltage capacitor bank charging.

TABLE I – Experimental Prototype Parameters

Parameter	*Value/Type*
Input voltage V_{in}	12V
Nominal output voltage V_{nom}	300V
Maximal output Power P_{max}	250W
Transistors	Vishay SUM90142E
Boost inductor L_B	22µH
Link inductor L_M	22µH
Flying capacitors C_B C_M	22 µF
Output capacitance C_{out}	110µF

has been built and tested. The MMHBC converter operates at 300kHz and is rated for maximum output power of 250W, the rest of the converter parameters are shown in Table I.

The digital controller has been implemented on a Microchip dsPIC33CK64MP103 alongside its analog front-end circuitry. Fig. 6 shows the experimental prototype setup, which comprises a four-phase MMHBC designed for maximum power of 250W and output voltage up to 350V. The converter phases are compact to provide increased overall power density of 2.5kW/Liter and minimize the overall system. The small converter also minimizes the differences between the phases routing and the resultant parasitic components within the system. The replicated structure of the phases also induces the system design procedure and reduce the complexity of designing higher phase count converters. The phase replication also equalizes the per-phase parasitic components and cuts down system losses.

The steady-state operation of the full MMHBC converter is shown in Fig. 7. Here, the transistor currents of phases 1 (i_{M1}) and 3 (i_{M3}) is shown alongside their corresponding PWM signals. The currents are measured by a Rogowski current probe and demonstrate good current sharing and phase interleaving of half switching cycle. The transistor currents are inherently balanced due to the current balancing capabilities of the ACM controller, this contributes to obtain excellent thermal balancing between the phases. As can be seen, the output voltage is 300V at maximum output power of 250W.

The capacitor charging experimental results are shown in Fig. 8. A 5mF capacitive bank is charge to 350V ($v_{out\ one}$, $v_{out\ two}$) using a two-stage and a single-stage converter. The two configurations operate at rated power throughout the charging phase as indicated by the enable signals (EN_{one}, EN_{two}). The single-stage converter achieves a full charge duration of 900ms in comparison to the two-stage case of 500ms. The difference in charging times correlates to the maximal input current obtainable within the duty cycle limitations. The two-stages converter operates with an average total input current ($i_{in\ two}$) of 18A (216W), drawing double current ($i_{in\ one}$) of the single stage case (9A, 108W). As mentioned in previous sections, a two-level system reduces the stress on the components and thus able to provide higher output power which accelerate the charging of the capacitive bank.

Fig. 9, demonstrates the operation of the MMHBC during phase shedding procedure, controlled by the system governor. The converter transition from four-phase operation to two-phase, due to low output power required during steady-state. Due to probing limitations, only phases 3 and 4 transistor currents are shown. The phase shedding enable indicator marks the time instance, and the controller shed phases 2 and 4, aiming to enhance the overall efficiency of the system. The instantaneous phase shedding procedure has a neglectable impact on the converter's output voltage regulation. This is achieved due to the decoupling effect of the additional amplification stages of the hybrid boost topology.

Fig. 10 shows the measured efficiency curves of the proposed converter with one and two amplification stages. It can be seen that a dual amplification stage operation yields a higher efficiency compared to this topology with a single amplification stage throughout the entire loading range. As stated in [15], adding additional amplification stages can drastically reduce the converter duty cycle for the same overall voltage gain. As a result, the system conduction losses decrease, and therefore the overall efficiency increases for multistage converters with additional amplification stages. The reduction in the conduction losses further increases in multiphase systems due to the increased phase count as can be seen in Fig. 10.

V. Conclusion

A multiphase hybrid boost converter with digital current-programmed ACM controller has been introduced and demonstrated using a four-phase experimental prototype. The digital controller is realized based on a dual-loop ACM control scheme with inherent current balancing capabilities. The MMHBC controller can operate in both constant current charging mode and constant voltage mode according to its target application. Phase shedding, soft-start, and protection features have been implemented to facilitate multiphase operation with enhanced performance. A 12V-to-300V four phase MMHBC experimental prototype has been built and tested for a maximum power rating of 250W, power density of 2.5kW/Liter.

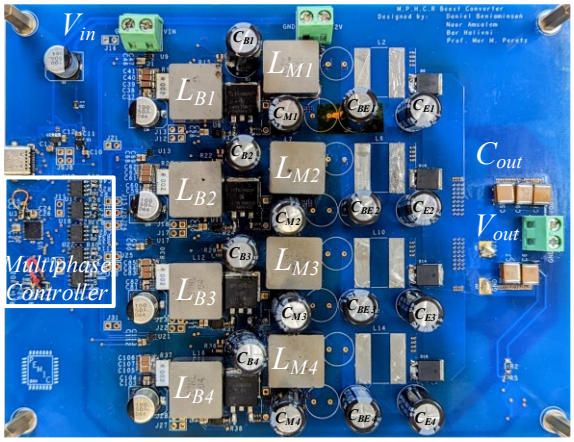

Fig. 6. Four-phase 12V-to-300V MMHBC experimental setup, including all the front-end peripherals and digital controller.

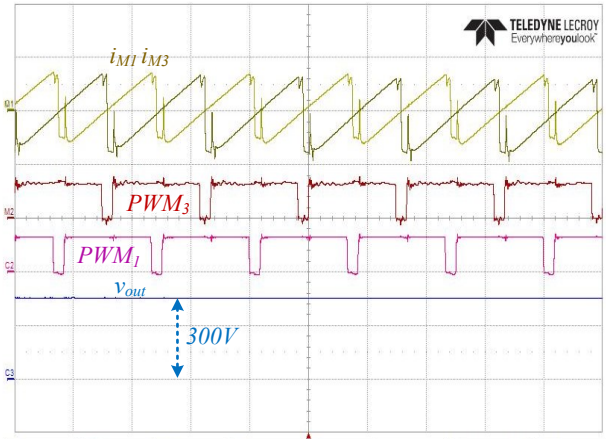

Fig. 7. Four-phase operation of the converter at constant voltage mode and output voltage of 300V (Gain = 25, Pout = 250W). i_{M_1}, i_{M3}(500mA/div), PWM_1, PWM_3(5V/div), v_{out}(200V/div).

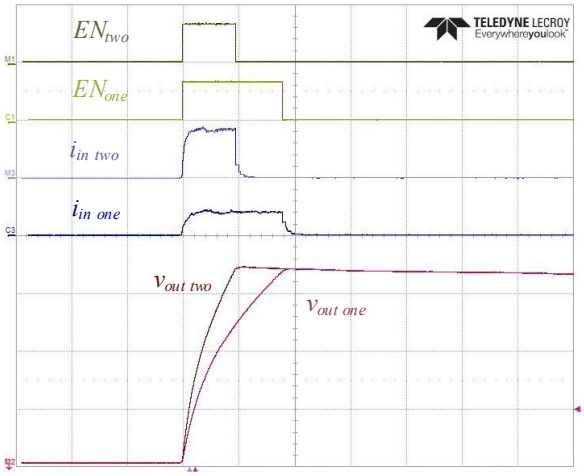

Fig. 8. Experimental waveforms of constant current capacitor bank charging for an output voltage of 350V through one and two amplification stages. EN_{one} , EN_{two} (5V/div), $i_{in\ one}$, $i_{in\ two}$ (20A/div), $v_{out\ one}$, $v_{out\ two}$ (100V/div).

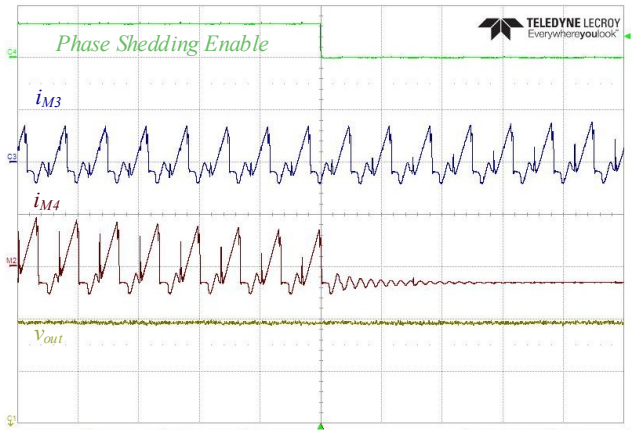

Fig. 9. Phase shedding operation during the transition from four to two phases. i_{M3}, i_{M4}(200mV/div), v_{out} (10V/div).

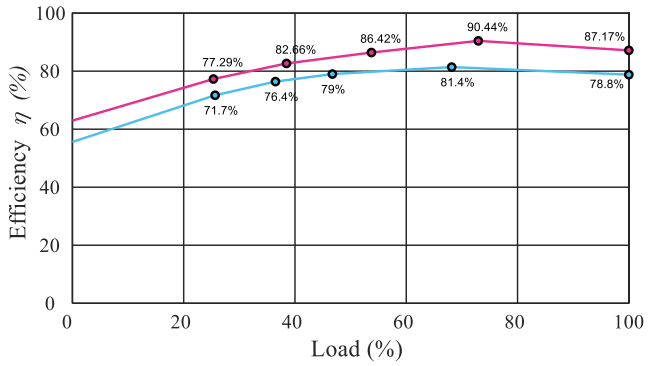

Fig. 10. Efficiency curves of four-phase operation of the converter at an input voltage of 12V and output voltage of 300V (when full-load obtained at 250W). Top – two amplification stage. Bottom – one amplification stages.

ACKNOWLEDGMENTS

This research was funded by the Israel Science Foundation under grant 2186/19, and by the Israel Ministry of Energy.

REFERENCES

[1] Z. Liao, Y. Lei, R. C. N. Pilawa-Podgurski, "Analysis and Design of a High Power Density Flying-Capacitor Multilevel Boost Converter for High Step-Up Conversion," IEEE Transactions on Power Electronics, vol. 34, no. 5, pp. 4087-4099, 2019.

[2] A. M. Naradhipa, S. Kim, D. Yang, S. Choi, I. Yeo, Y. Lee, "Power Density Optimization of 700 kHz GaN-Based Auxiliary Power Module for Electric Vehicles," IEEE Transactions on Power Electronics, vol. 36, no. 5, pp. 5610-5621, 2021.

[3] M. A. Rezaei, K. -J. Lee, A. Q. Huang, "A High-Efficiency Flyback Micro-inverter With a New Adaptive Snubber for Photovoltaic Applications," IEEE Transactions on Power Electronics, vol. 31, no. 1, pp. 318-327, 2016.

[4] X. Cao, W. Chiang, Y. King, Y. Lee, "Electromagnetic Energy Harvesting Circuit With Feedforward and Feedback DC–DC PWM Boost Converter for Vibration Power Generator System," *IEEE Transactions on Power Electronics*, vol. 22, no. 2, pp. 679-685, 2007.

[5] H. Lee ,J. Yun, "Quasi-Resonant Voltage Doubler With Snubber Capacitor for Boost Half-Bridge DC–DC Converter in Photovoltaic Micro-Inverter," *IEEE Transactions on Power Electronics*, vol. 34, no. 9, pp. 8377-8388, 2019.

[6] B. Balachander, S. Sinthamani and S. Sudharsanam, "Solar Powered DC - DC Converter for Wearable Devices," *International Conference on Electrical Energy Systems* , pp. 425-432, 2018.

[7] A. Dionisi, D. Marioli, E. Sardini, M. Serpelloni, "Autonomous Wearable System for Vital Signs Measuremennt With Energy-Harvesting Module", *IEEE Transaction on Instrumentation and Measurement Society*, vol. 65, no. 6, pp. 1423-1434, 2016.

[8] S. Jain, B. S. Satish, J. -S. J. Lai, "High gain resonant boost converter for PV micro-converter system," *IEEE Energy Conversion Congress and Exposition*, pp. 1-6, 2016.

[9] T. LaBella, W. Yu, J.S. Lai, M. Senesky, D. Anderson, "Bidirectional-Switch-Based Wide-Input Range High-Efficiency Isolated Resonant Converter for Photovoltaic Applications", *IEEE Transactions on Power Electronics*, vol. 29, no. 7, pp. 3473-3484, 2014.

[10] T. LaBella, J.-S. Lai, "A Hybrid Resonant Converter Utilizing a Bidirectional GaN AC Switch for High-Efficiency PV Applications", *IEEE Transactions on Industry Applications*, vol. 50, no. 5, pp. 3468-3475, 2014.

[11] M. Forouzesh, A. Baghramian, "High voltage gain Y-source based isolated DC-DC converter with continuous input current", *Power Electronics Drives Systems & Technologies Conference*, pp. 453-457, 2015.

[12] R. Pittini, Z. Zhang, M. A. E. Andersen, "Isolated full bridge boost DC-DC converter designed for bidirectional operation of fuel cells/electrolyzer cells in grid-tie applications," *European Conference on Power Electronics and Applications*, pp. 1-10, 2013.

[13] Q. Zhao, F. C. Lee, "High-efficiency, high step-up DC-DC converters," *IEEE Transactions on Power Electronics*, vol. 18, no. 1, pp. 65-73, 2003.

[14] L. Qin, L. Zhou, W. Hassan, J. L. Soon, M. Tian, J. Shen, "A Family of Transformer-Less Single-Switch Dual-Inductor High Voltage Gain Boost Converters With Reduced Voltage and Current Stresses," *IEEE Transactions on Power Electronics*, vol. 36, no. 5, pp. 5674-5685, 2021.

[15] V. K. Rathore, M. Evzelman, M. M. Peretz, "Non-Isolated High Conversion Ratio Boost Extender Based on Back-end Series Capacitor Stacking," *IEEE Workshop on Control and Modeling for Power Electronics*, pp. 1-7, 2022.

[16] Z. Lukic, Z. Zhao, A. Prodic, D. Goder, "Digital Controller for Multi-Phase DC-DC Converters with Logarithmic Current Sharing," *IEEE Power Electronics Specialists Conference*, pp. 119-123, 2007.

[17] S. Chae, Y. Song, S. Park, H. Jeong, "Digital Current Sharing Method for Parallel Interleaved DC–DC Converters Using Input Ripple Voltage," *IEEE Transactions on Industrial Informatics*, vol. 8, no. 3, pp. 536-544, 2012.

[18] M. M. Jovanovic, D. E. Crow, L. Fang-Yi, "A novel, low-cost implementation of "democratic" load-current sharing of paralleled converter modules," *IEEE Transactions on Power Electronics*, vol. 11, no. 4, pp. 604-611, 1996.

[19] Y. Su, K. -Y. B. Cheng, W. Wu, "High-efficiency multiphase DC-DC converters for powering processors with turbo mode based on configurable current sharing ratios and intelligent phase management," *IEEE Applied Power Electronics Conference and Exposition*, pp. 191-196, 2017.

[20] S.-H. Baek, S.-R. Lee, C.-Y. Won, "A novel phase shedding control algorithm considering maximum efficiency for 3-phase interleaved boost converter," *IEEE Transportation Electrification Conference and Expo*, pp. 427-431, 2016.

[21] Y. Ahn, I. Jeon, J. Roh, "A Multiphase Buck Converter With a Rotating Phase-Shedding Scheme For Efficient Light-Load Control," *IEEE Journal of Solid-State Circuits*, vol. 49, no. 11, pp. 2673-2683, 2014.

[22] S. Nahar, M. B. Uddin, "Analysis the performance of interleaved boost converter," *International Conference on Electrical Engineering and Information & Communication Technology*, pp. 547-551, 2018.

[23] Y. Hsieh, T. Hsueh, H. Yen, "An Interleaved Boost Converter With Zero-Voltage Transition," *IEEE Transactions on Power Electronics*, vol. 24, no. 4, pp. 973-978, 2009.